

Review and Recommended Experimental Procedures for Evaluation of Abrupt-Wing-Stall Characteristics

Francis J. Capone,* Robert M. Hall,† D. Bruce Owens,‡ John E. Lamar,§ and S. Naomi McMillin¶
NASA Langley Research Center, Hampton, Virginia 23681

A review of the experimental program for four different aircraft configurations conducted as part of the Abrupt Wing Stall Program has been made. Several candidate figures of merit from conventional static-tunnel tests are summarized and correlated with data obtained in unique free-to-roll tests. The conclusion from this study is that these figures of merit can by themselves give some indication as to whether an aircraft would experience uncommanded lateral activity caused by abrupt wing stall. However, no one specific figure of merit consistently flagged a warning of potential lateral activity when actual activity was seen to occur in the free-to-roll experiments. In fact, they yielded as many or more false indications of lateral activity than were seen in the free-to-roll response data. Excellent agreement between free-to-roll results and flight was obtained for those configurations where flight data were available.

Nomenclature

| | | |
|---------------|---|---------------------------------------|
| C_L | = | lift coefficient |
| C_{LWB} | = | left-wing bending-moment coefficient |
| C_l | = | rolling-moment coefficient |
| $C_{l,rms}$ | = | rms of C_l |
| $C_{N,rms}$ | = | rms of normal-force coefficient |
| C_{RWB} | = | right-wing bending-moment coefficient |
| M | = | Mach number |
| α | = | angle of attack, deg |
| δ_a | = | aileron angle, deg |
| δ_{le} | = | leading-edge flap angle, deg |
| δ_{te} | = | trailing-edge flap angle, deg |
| θ | = | model pitch angle, deg |
| ϕ | = | model roll angle, deg |

Introduction

A JOINT NASA/Navy/Air Force Abrupt Wing Stall Program (AWS) was established after several preproduction F/A-18E/F aircraft experienced severe wing-drop motions during the development stage. A Blue Ribbon Panel determined that a poor understanding of the phenomena causing the problem existed and made the recommendation to “initiate a national research effort to thoroughly and systematically study the wing drop phenomena.” The problem area addressed by the AWS Program¹ is the unexpected occurrence of highly undesirable lateral-directional motions at high-subsonic and transonic maneuvering conditions. One of the recommendations made by Chambers and Hall² was “to define and assess candidate figures of merit for the prediction of wing drop and wing rock from experimental methods.”

The interpretation of experimental data obtained in wind tunnels for conditions involving highly separated wing flows has always been very subjective and open to many opinions as to what is happening. One aircraft that went through an extensive experimental

program because of uncommanded wing rock/drop was the Harrier³ aircraft, where the potential existence of wing rock/drop was interpreted from wind-tunnel rolling-moment data.

An extensive experimental wind-tunnel test program has been conducted as part of the AWS program. One of the objectives of the AWS program was to test four different aircraft that are known to either exhibit uncommanded lateral motions or not. The preproduction F/A-18E and AV-8B were chosen because these two aircraft exhibited wing-drop behavior. The two configurations that did not have wing drop were the F/A-18C and the F-16C. The overall geometric dimensions of these models are shown in Fig. 1 as well as a summary of the scope of experimental measurements made in the program. Free-to-roll testing was accomplished using the test technique described in Ref. 4.

This paper will summarize the candidate figures of merit from conventional static-tunnel tests and review how well they correlate with data obtained in unique free-to-roll tests. Where possible, free-to-roll results are also correlated with flight data. Recommendations as to how to conduct an experimental program on future vehicles are made.

Static Forces and Figures of Merit

One question that arose during the AWS Program was whether one could rely solely on figures of merit derived from static data taken during a transonic model test to provide the certainty needed that a new aircraft would or would not be susceptible to uncommanded lateral motions during its flight operations. Static figures of merit (FOMs) are very important because they are intended to predict wing-drop/rock behavior and, consequently, will enter into the decision of doing free-to-roll testing or not. Comparing static test results with the free-to-roll (FTR) response data has provided a rational basis for assessing the merits of using standard test techniques for the prediction of AWS events.

The traditional figures of merit (TFOMs) from static wind-tunnel tests include the lift-curve break and asymmetries in the variation of rolling-moment coefficient C_l and rms of rolling moment $C_{l,rms}$ with angle of attack. Experience has taught that changes in these parameters can be indicative of changes in flow topology that can lead to the kinds of aircraft response denoted as abrupt wing stall flight events. Any discontinuities in the slope of lift curve reflect changes in the flow physics and can be indicative of buffet onset, wing drop, wing rock, or loss of roll damping. Reference 5 questioned whether any lift beyond the kink “is usable” for nonlinear curves. The rationale for considering asymmetries in rolling moment is that uncommanded lateral motions are the result in flight of one wing stalling before the other and can be captured in the wind tunnel by examining rolling moments.³

Presented as Paper 2003 at the AIAA 41st Aerospace Sciences Meeting and Exhibit, Reno, NV, 6 January 2003; received 30 May 2003; revision received 15 August 2003; accepted for publication 10 September 2003. This material is declared a work of the U.S. Government and is not subject to copyright protection in the United States. Copies of this paper may be made for personal or internal use, on condition that the copier pay the \$10.00 per-copy fee to the Copyright Clearance Center, Inc., 222 Rosewood Drive, Danvers, MA 01923; include the code 0021-8669/04 \$10.00 in correspondence with the CCC.

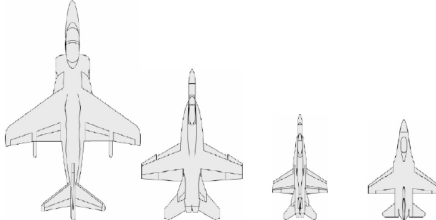
*Senior Research Engineer.

†Senior Research Engineer. Associate Fellow AIAA.

‡Aerospace Engineer. Member AIAA.

§Aerospace Engineer. Member AIAA.

¶Senior Research Engineer. Associate Fellow AIAA.

Fig. 1 Scope of AWS investigations.


| Parameter | AV-8B | F-18E/F | F-18C | F-16C |
|--------------------------------|-------|---------|-------|-------|
| Length, in. | 81.27 | 54.99 | 39.18 | 37.25 |
| Wing area, ft ² | 5.18 | 3.2 | 1.33 | 1.67 |
| Span, ft | 4.55 | 3.34 | 2.25 | 2.07 |
| Weight, lbs | 490 | 185 | 55 | 56 |
| Inertia, slugs-ft ² | 4.0 | 1.2 | 0.2 | 0.2 |
| Scale, % | 15 | 8 | 6 | 6.67 |
| F & M | Yes | Yes | Yes | Yes |
| F & M, rms | Yes | Yes | Yes | Yes |
| WB | Yes | Yes | No | No |
| WB, rms | Yes | Yes | No | No |

During the AWS program and prior to the acquisition of any free-to-roll results, questions arose as to whether the traditional figures of merit would work with 100% accuracy with no misses.⁶ Consequently, alternate figures of merit (AFOMs) were considered to see if they would offer any predictive improvements. The AFOMs considered occur in two different classes, steady and unsteady, where both use combinational forms of measured parameters to help distinguish between AWS and non-AWS events. The steady group deals with the derivative form of basic aerodynamic terms, whereas the unsteady group incorporates the rms components of selected aerodynamic terms and are only considered herein. The rms weighted sum alternate figures of merit are

$$\Sigma\text{FOM}_{22} = \sqrt{(C_{l,rms}^2 + C_l^2)/2}$$

and

$$\Sigma\text{FOM}_{33} = \sqrt{(C_{N,rms}^2 + C_{l,rms}^2 + C_l^2)/3}$$

where ΣFOM_{22} and ΣFOM_{33} are summation figures of merit.

An AFOM that is the absolute value of a simple product is defined as

$$\Pi\text{FOM} = |C_{N,rms} \times C_{l,rms} \times \Delta C_l|$$

where the term ΔC_l is used to remove any offset in rolling-moment coefficient at low angles of attack and ΠFOM is a product figure of merit. For this figure of merit, an AWS event was predicted to occur if the value of ΠFOM remained above a level established during early testing of the preproduction F/A-18E. This level was found useful in sorting model configurations from different wind tunnels.

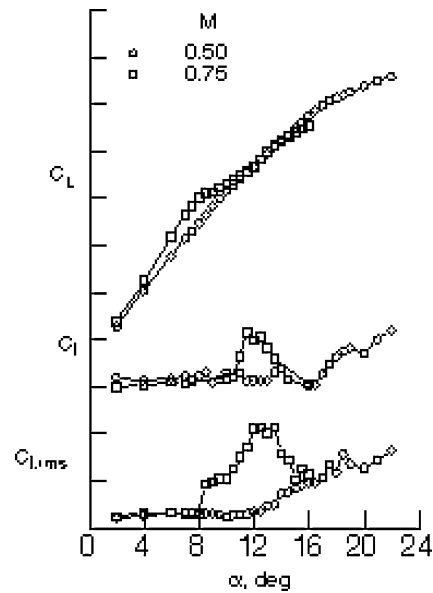
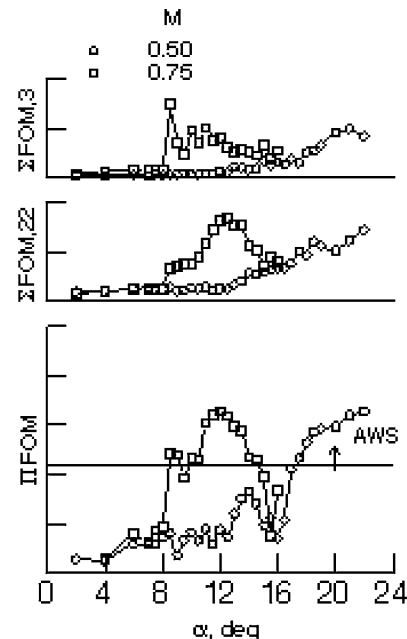
One is now faced with the problem of defining criteria that are indicative of the occurrence of an AWS event. Sharp breaks in lift-curve slope have traditionally been used as an indicator of an abrupt stall, which because of its nature can be asymmetric. Sudden or rapid variations in either rolling-moment coefficient or rms of rolling moment can signify rapid flow topology changes as angle of attack changes. The angle of attack at which these curves have a spike or peak is used as the criteria to indicate AWS activity for the FOMs considered. However, as will be shown, where AWS activity is initiated is a matter of conjecture, and it could be argued that this activity starts at some angle of attack prior to that indicated by the spike or peak. For those cases in which wing bending moments were measured, a reversal in the slope of these curves is used as the criteria.

Example results for the four models are presented to show when both traditional (TFOMs) and alternate (AFOMs) figures of merit indicated that AWS activity would be present and also where these figures of merit indicated some activity would be present but was not.

Angles of attack at which a figure of merit such as lift-curve break would predict some AWS activity would be present are summarized in a “stoplight” chart. The stoplight chart also presents color-coded results measured during the pitch-pause phase of free-to-roll testing. During FTR pitch-pause tests,⁴ the model was released from a wings-level condition, and the resulting motions were recorded. A discussion of the color-coded rating system is given in the free-to-roll figure of merit section of this paper. The notation “flaps on schedule” appearing on some of the figures of this paper indicate the flap settings that the full-scale aircraft would be flying at the specified Mach number and α or θ .

AV-8B

Four configurations of the AV-8B have been selected for discussion, based on trailing-edge flap deflection, LERX, and Mach number combinations. The TFOMs and AFOMs are presented in Figs. 2–5 and compared to flight and FTR results in Figs. 6 and

**Fig. 2 Traditional figures of merit for AV-8B: 100% LERX, and $\delta_{te} = 10$ deg.****Fig. 3 Alternate figures of merit for AV-8B: 100% LERX, and $\delta_{te} = 10$ deg.**

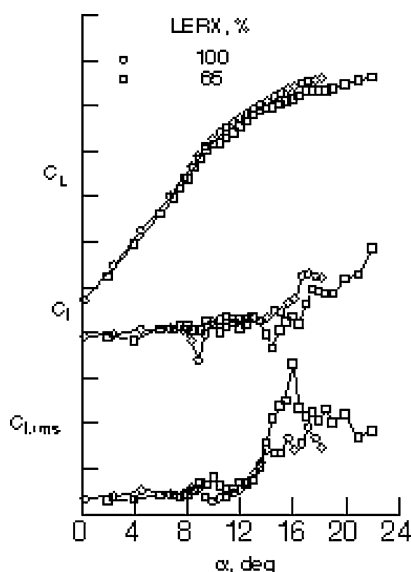


Fig. 4 Traditional figures of merit for AV-8B: $\delta_{te} = 25$ deg, and $M = 0.50$.

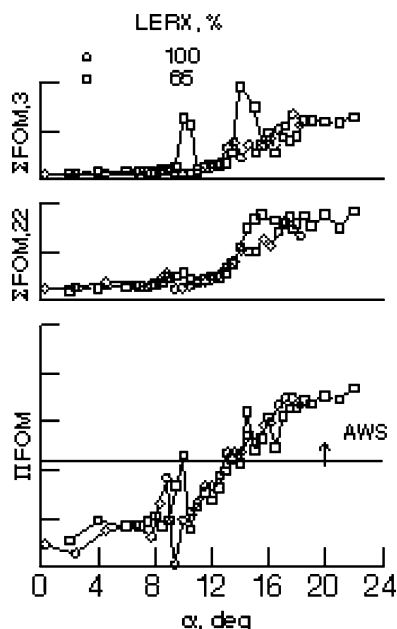


Fig. 5 Alternate figures of merit for AV-8B: $\delta_{te} = 25$ deg, and $M = 0.50$.

7. Data shown on the stoplight charts are presented as a function of model pitch angle θ rather than angle of attack because during FTR testing θ can be held constant, whereas angle of attack α varies during the model rolling motions. When α or $\theta = 0$ deg, these angles differ only by tunnel upflow angularity that averaged about $+0.10$ deg.

There is a marked difference in the magnitude of the breaks in the lift curves between a Mach number of 0.50 and 0.75 for the AV-8B with the 10-deg trailing-edge flap (Fig. 2). At $M = 0.50$, there is a slight decrease in the lift-curve slope at $\alpha = 7.5$ deg, whereas at $M = 0.75$ a much sharper decrease in slope exists at $\alpha = 8.5$ deg. Because breaks in C_L curves could be indicative of AWS activity, this is one of the conditions noted on the stoplight chart of Fig. 6. In addition, several other static figures of merit indicated the potential for AWS activity at or near this angle of attack. These included $\Sigma FOM,3$, ΠFOM , wing-bending moments, and the computational-fluid-dynamics (CFD)-predicted C_L break. However, as can be seen in Fig. 6, although more than half of the FOMs predicted AWS activity the free-to-roll results showed no lateral activity in this angle

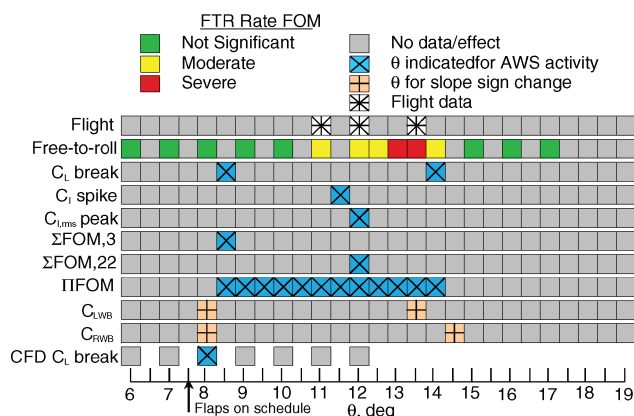


Fig. 6 Stoplight chart for AV-8B: 100% LERX, $\delta_{te} = 10$ deg, and $M = 0.75$.

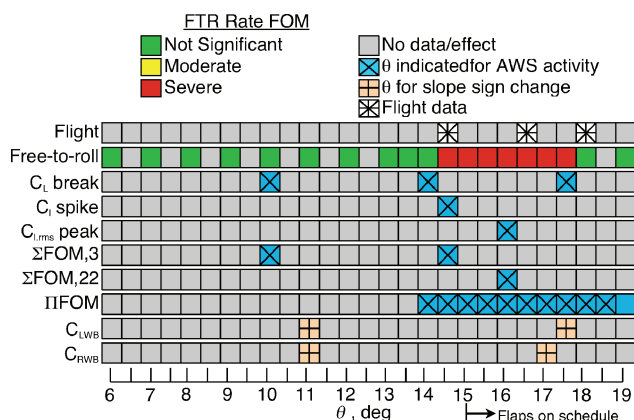


Fig. 7 Stoplight chart for AV-8B: 65% LERX, $\delta_{te} = 25$ deg, and $M = 0.50$.

of attack range. Figure 2 also shows a difference in the character of rolling-moment coefficient between $M = 0.5$ and 0.75. At $M = 0.5$, no FTR lateral activity was seen, despite the sharp increase in rolling moment indicated in Fig. 2 at $\alpha = 16$ deg. However, the very large asymmetries in rolling moment present at $M = 0.75$ are more typical of the behavior one can expect where uncommanded lateral motions might be present and, in fact, were experienced during the FTR tests (Fig. 6). Also shown in Fig. 6 is the CFD prediction⁷ of the break in the lift curve at $M = 0.75$, where good agreement is noted between the prediction and experiment. Although not shown, the predicted break in lift-curve slope at $M = 0.50$ occurred about 3 deg higher than that measured.

Several of the figures of merit predict AWS activity for the AV-8B at $M = 0.50$ with the 65% LERX (Fig. 7) at $\theta = 14$ –14.5 deg, and severe AWS activity was experienced in the FTR tests. Note that there were also false predictions of activity near $\alpha = 10$ deg. Wing rock occurred with flaps on schedule at θ greater than 14 deg.

For the AV-8B, both rolling moment and rolling-moment rms appear to be the significant figures of merit, and the results suggest that any future program include these measurements. The results of the static portion of the tests on the AV-8B also suggest a need to conduct FTR tests.

Preproduction F/A-18E

The traditional and alternate figures of merit for the F/A-18E with flap settings of 6 deg/8 deg/4 deg, 10 deg/10 deg/5 deg, and 15 deg/10 deg/5 deg at $M = 0.90$ are presented in Figs. 8 and 9 and summarized in Fig. 10. The first angle corresponds to leading-edge flap deflection, the second angle corresponds to the trailing-edge flap deflection, and the third angle corresponds to the aileron bias. The lift curves for the 6 deg/8 deg/4 deg and 10 deg/10 deg/5 deg flap settings have very significant breaks, similar to the F-18C. However,

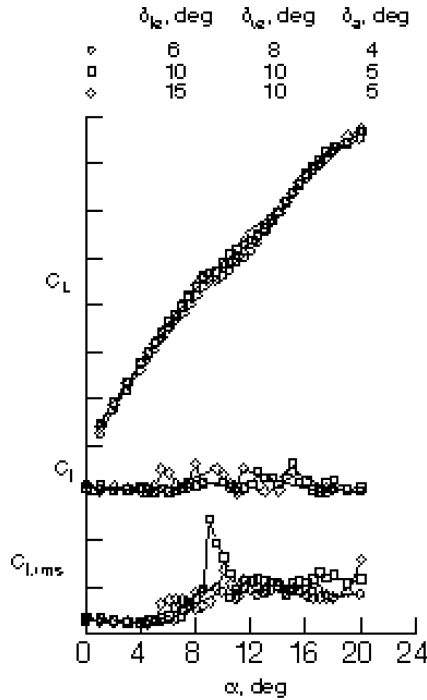


Fig. 8 Traditional figures of merit for preproduction F/A-18E: and $M = 0.90$.

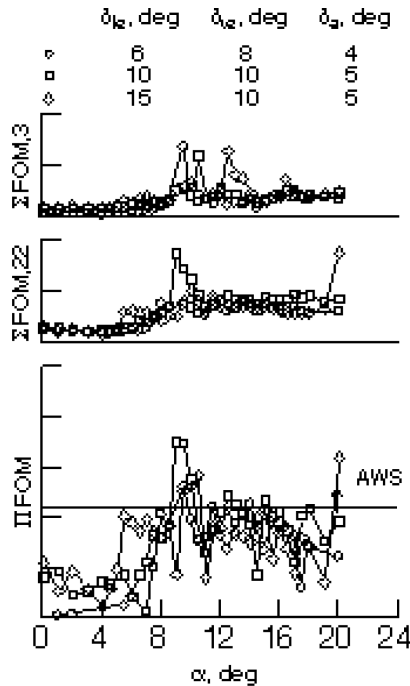


Fig. 9 Alternate figures of merit for preproduction F/A-18E: and $M = 0.90$.

FTR lateral activity was already present, having started some 1–1.5 deg sooner than what would have been predicted by the breaks in lift curves. For the 10 deg/10 deg/5 deg flap setting, all of the figures of merit including the CFD FOM⁸ line up and essentially predicted lateral activity. Even though the time-averaged C_L data indicate significant variation with α , the unsteady $C_{l,rms}$ data are smoother. Although FTR lateral activity is present with flaps on schedule, these results are for a model of the preproduction F/A-18E aircraft and are not representative of the production aircraft.¹ For this configuration, lift-curve slope and rolling moment tended to predict AWS activity at angles of attack higher than where FTR lateral activity was present except at $\theta = 18$ deg, where no FTR was

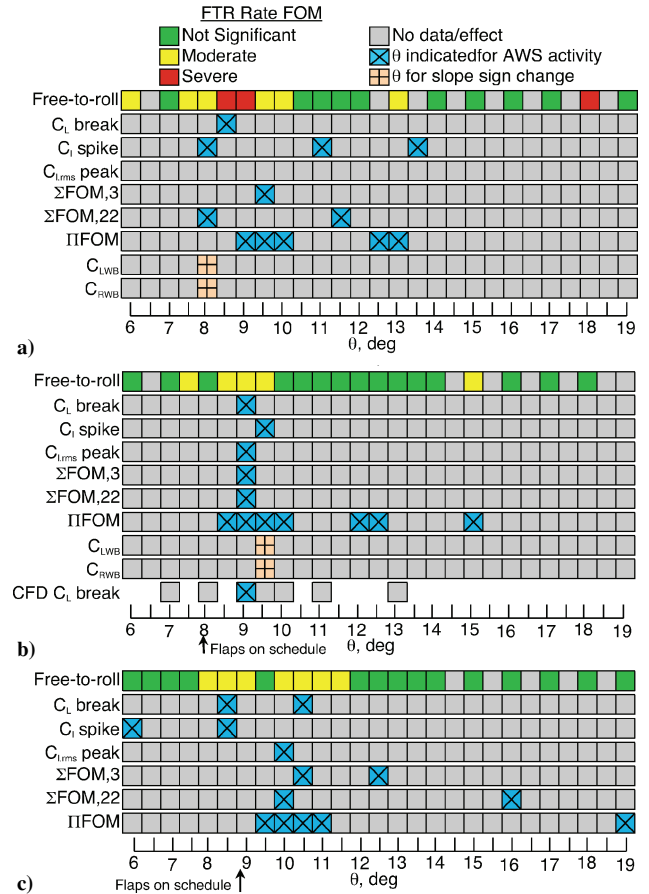


Fig. 10 Stoplight chart for F/A-18E, $M = 0.90$: a) $\delta_{le} = 6$ deg, $\delta_{le} = 8$ deg, $\delta_a = 4$ deg; b) $\delta_{le} = 10$ deg, $\delta_{le} = 10$ deg, $\delta_a = 5$ deg; and c) $\delta_{le} = 15$ deg, $\delta_{le} = 10$ deg, $\delta_a = 5$ deg.

predicted. However, in the absence of any FTR data, the results of the static portion of this investigation on the preproduction F/A-18E clearly show a need for FTR testing of this configuration.

F/A-18C

The traditional and alternate figures of merit for the F/A-18C with $\delta_{le} = 6$ deg, $\delta_{le} = 8$ deg, and $\delta_a = 0$ deg (6 deg/8 deg/0 deg) at $M = 0.80$ – 0.90 are presented in Figs. 11 and 12, respectively. The first angle corresponds to leading-edge flap deflection, the second angle corresponds to the trailing-edge flap deflection, and the third angle corresponds to the aileron bias. These data are summarized in Fig. 13. At all Mach numbers, there are very significant breaks in the lift curves that are in marked contrast to those shown for the AV-8B. Figure 13 indicates that severe FTR lateral activity occurred at angles for which the flaps are not on schedule for the full-scale F/A-18C aircraft. An examination of Fig. 13 suggests the difficulty predicting AWS activity from the TFOMs and AFOMs. At this Mach number and others not shown, the figures of merit sometimes reliably predicted activity, and sometimes they falsely predicted activity. Also shown in Fig. 13 are the CFD predictions⁷ of the break in the lift curve at $M = 0.85$ and 0.9 . As can be seen, the predicted break in lift-curve slope at $M = 0.90$ occurred about 1 deg lower than that measured.

For the F/A-18C configuration, lift-curve slope, rolling moment, and rms rolling moment appear to be significant FOMs, such that any future program should include these measurements.

F-16C

The traditional and alternate figures of merit for the F-16C with $\delta_{le} = 10$ deg and $\delta_{le} = 0$ deg at $M = 0.80$ and 0.90 are presented in Figs. 14 and 15 respectively, and summarized in Fig. 16. For the F-16C configuration, the TFOMs predicted that some AWS activity would be present, but no FTR lateral activity was present. This

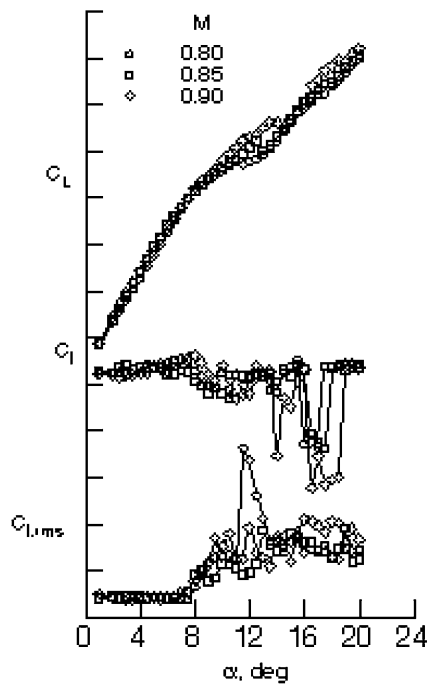


Fig. 11 Traditional figures of merit for F/A-18C: $\delta_{le} = 6$ deg, $\delta_{te} = 8$ deg, and $\delta_a = 0$ deg.

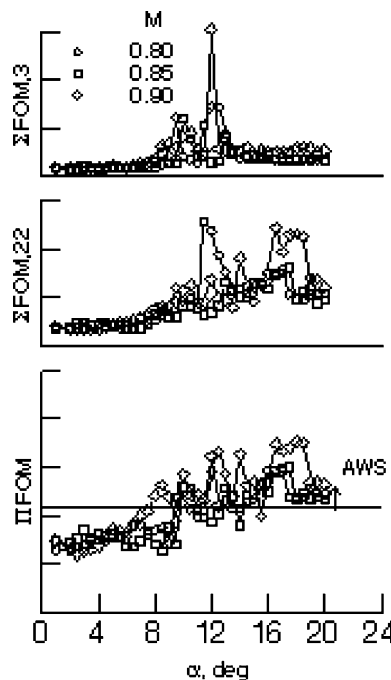


Fig. 12 Alternate figures of merit for F/A-18C: $\delta_{le} = 6$ deg, $\delta_{te} = 8$ deg, and $\delta_a = 0$ deg.

result was also seen for other combinations of flap settings and Mach numbers and again highlighted the lack of reliable FOMs because this was a configuration with no known wing-drop behavior. Although not shown, there were no breaks in the CFD predicted lift curves.⁸

Free-to-Roll to Flight Correlations

Free-to-Roll Figure of Merit

A figure of merit was also developed for free-to-roll testing in order to resolve levels of model lateral activity from inconsequential to “significant.” Taking into account amplitude alone could lead to the wrong conclusions because the motion might have a large ampli-

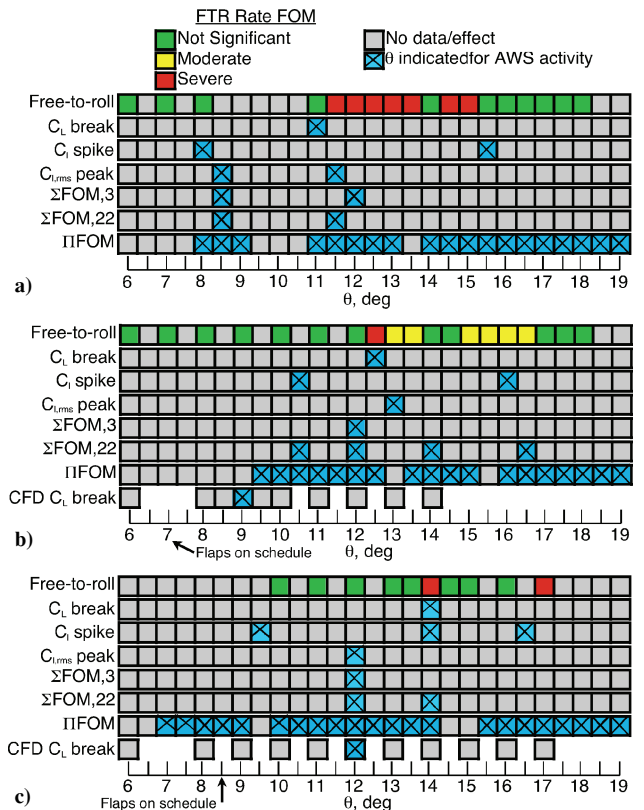


Fig. 13 Stoplight chart for F/A-18C: $\delta_{le} = 6$ deg, $\delta_{te} = 8$ deg, and $\delta_a = 0$ deg; a) $M = 0.80$, b) $M = 0.85$, and c) $M = 0.90$.

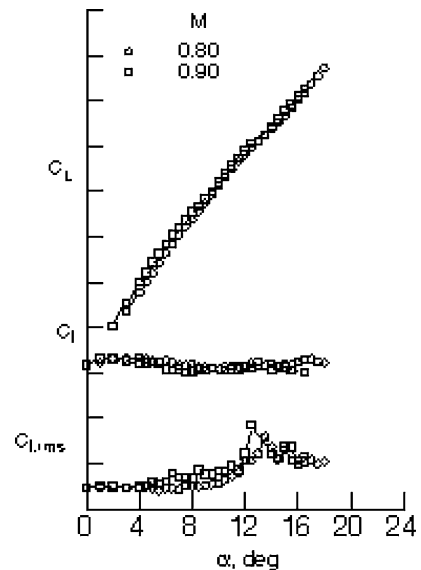


Fig. 14 Traditional figures of merit for F-16C: $\delta_{le} = 10$ deg, and $\delta_{te} = 0$ deg.

tude change but be so slow that it would be easily controlled. Taking into account just the magnitude of rates or accelerations alone could also lead to the wrong conclusions because a large acceleration with small amplitude oscillation might not be controllable but would not lead to a large deviation in the aircraft trajectory. Or, the acceleration might be favorable if it is returning the aircraft to a wings-level condition.

Initially, only amplitude measured during pitch-pause free-to-roll testing⁴ was used as a figure of merit. During FTR pitch-pause tests, the model was released from a wings-level condition, and the resulting motions were assigned an arbitrary color-coded rating. This system was based on the ensuing amplitude of bank angle,

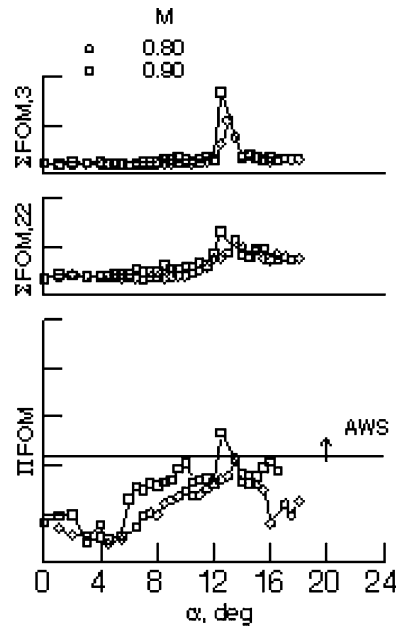


Fig. 15 Alternate figures of merit for F-16C: $\delta_{lc} = 10$ deg, and $\delta_{te} = 0$ deg.

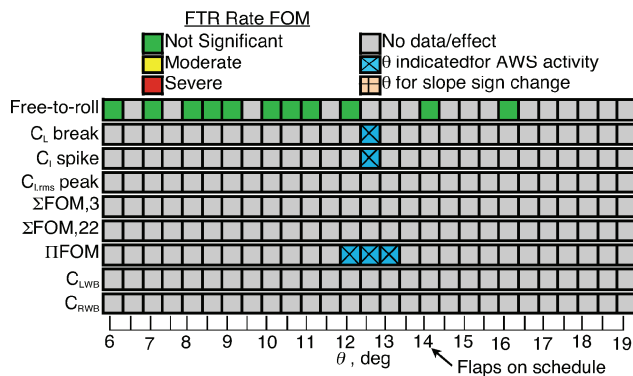


Fig. 16 Stoplight chart for F-16C: $\delta_{lc} = 10$ deg, $\delta_{te} = 0$ deg, and $M = 0.90$.

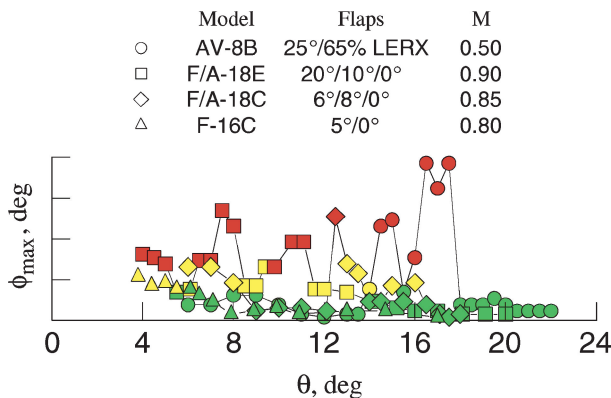


Fig. 17 Initial ratings for selected configurations tested.

where green represented an amplitude of less than 10 deg, yellow an amplitude between 10 and 20 deg and red any amplitude greater than 20 deg. Initial ratings for a selected configuration of each of the four models tested are presented in Fig. 17. Note the large number of yellow and red events that occur for the F/A-18E and F/A-18C at low angles of attack. These events are generally slow-period large-amplitude motions and are not considered to be either wing drop or rock events.

Therefore, a new figure of merit⁹ was developed that accounted for both amplitude and rate. The FTR rate FOM is defined as the maximum absolute value of the amplitude change from a peak to its nearest valley divided by the time it takes to roll through this amplitude. This method captures wing drops that have no overshoots and wing rock that has sinusoidal motion. A color-coded system was also devised for this FOM, where green represented values less than 50, yellow had values between 50 and 100, and red any value greater than 100. Although still somewhat arbitrary, the various levels were established after a review of all of the results from the four models showed data falling predominately within these three bands.

The current ratings for the same four configurations shown in Fig. 17 are presented in Fig. 18. Although the same range is used for all of the models, there is no expectation that the level of lateral activity means the same for all airplanes given their different sizes and inertias. As can be seen, the preceding the low θ red (severe events) for the preproduction F/A-18E have now become green (not significant) events. Also note that the green event occurring at $\theta = 15.5$ deg for the AV-8B (Fig. 17) has become a red event, which give a more consistent story in that θ range.

Roll-Rate Correlation

A correlation of roll-rate to roll-acceleration has been performed for each of the four configurations tested during the FTR tests, and these results are presented in Fig. 19. All data collected during the

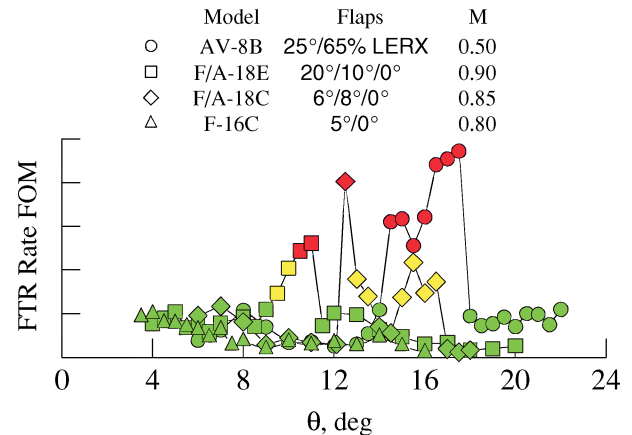


Fig. 18 Final ratings for selected configurations tested.

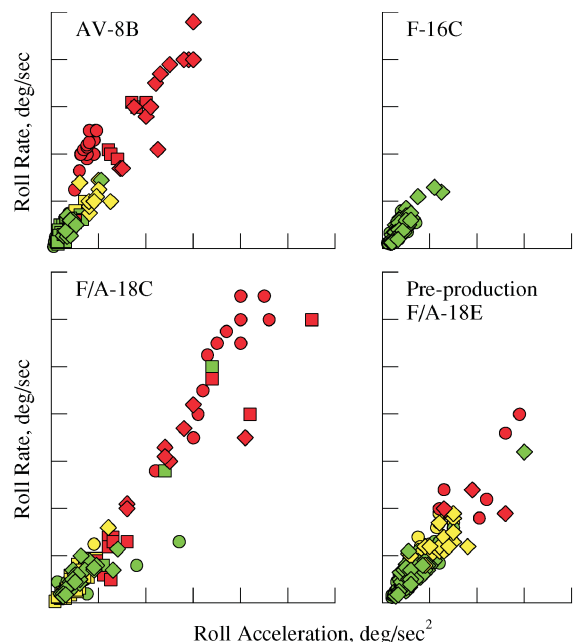


Fig. 19 Roll-rate characteristics for the four configurations.

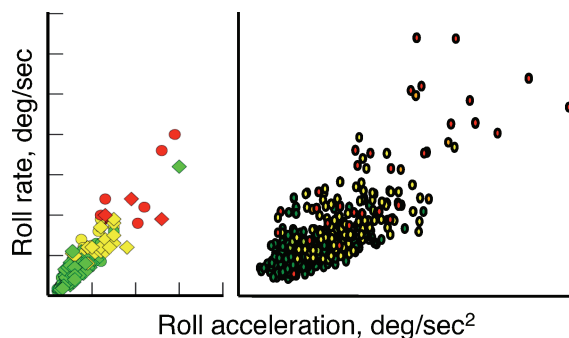


Fig. 20 Free-to-roll/flight comparison of preproduction F/A-18E roll rates.

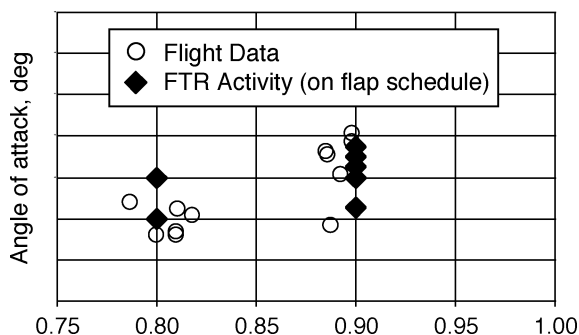


Fig. 21 Free-to-roll/flight comparison for preproduction F/A-18E.

pitch-pause phase of the FTR tests are given for each configuration. Note that all configurations have been plotted to the same scales. The highest roll rates measured were for the F-18C at angles of attack in which the flaps were off schedule.

Roll rates for the F/A-18E determined in the wind tunnel and flight¹⁰ are shown in Fig. 20. A direct comparison of these wind-tunnel and flight data cannot be made because the wind-tunnel model was not dynamically scaled to the aircraft, and the aircraft stability augmentation system was not represented in the FTR test technique. However, the trends of roll-rate variation with acceleration are very similar.

Angle-of-Attack Correlation

A comparison of FTR activity to flight data for the preproduction F/A-18E is shown in Fig. 21 for Mach numbers of 0.8 and 0.9. The data shown are where both the airplane and model had approximately the same flap settings and Mach number at the time of a lateral activity event. As can be seen, there is good agreement between wind tunnel and flight. However, this correlation only shows unacceptable lateral activity, not the type of lateral activity. Although FTR lateral activity is present with flaps on schedule, these results are for a model of the preproduction F/A-18E aircraft¹ and are not representative of the production aircraft.¹

Figures 22 and 23 show a comparison of angles of attack for wing rock/drop between flight and wind tunnel for the AV-8B with the 100% and the 65% LERX. Flight data for the 100% LERX are only available for Mach numbers greater than 0.5, whereas flight data exist for the 65% LERX at Mach numbers from about 0.22–0.90. The ranges of wind-tunnel data presented are for yellow or red conditions. As can be seen, there is excellent agreement between the flight and wind-tunnel data. Any wing-drop/rock activity noted is not considered an AV-8B aircraft operational problem.

Roll-Damping Correlation

A correlation of roll damping between flight¹¹ and those measured in the wind tunnel are presented in Fig. 24. Roll damping is extracted from the roll-angle time histories of the resulting motions when the model is released from some initial roll angle. Good agreement is

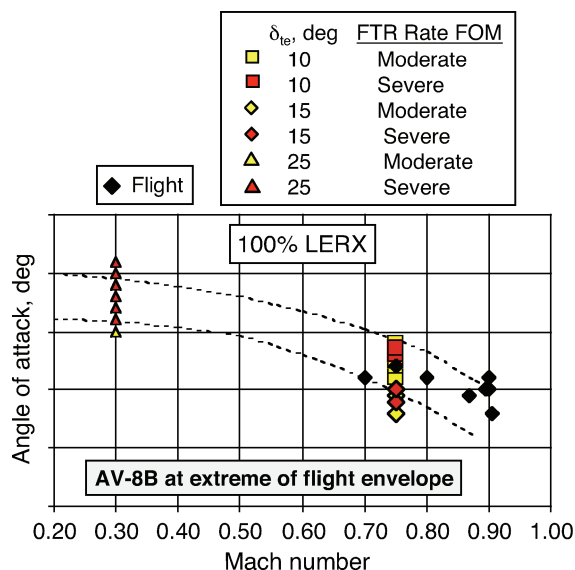


Fig. 22 Free-to-roll/flight comparison for AV-8B: 100% LERX.

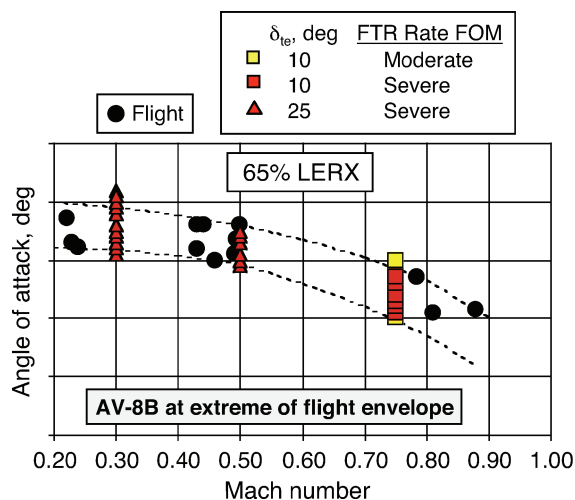


Fig. 23 Free-to-roll/flight comparison for AV-8B: 65% LERX.

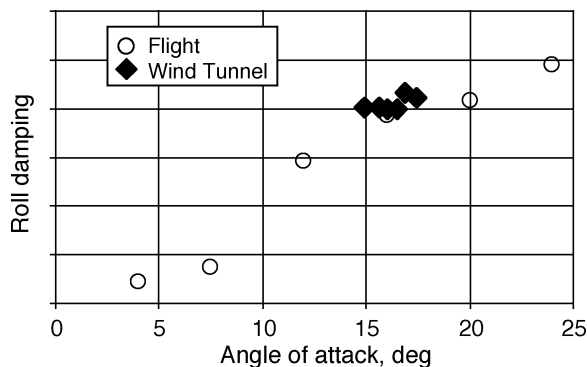


Fig. 24 Free-to-roll/flight comparison of AV-8B roll damping.

noted in Fig. 24. An analysis of the time histories indicated that the severe wing rock the AV-8B experienced at $M = 0.50$ resulted from a loss of roll damping.⁹

Summary

A review of the experimental program for four different aircraft configurations conducted as part of the Abrupt Wing Stall Program has been made. Several candidate figures of merit from conventional static-tunnel tests are summarized and correlated with

data obtained in unique free-to-roll tests. The conclusion from this study is that these figures of merit can by themselves give some indication as to whether an aircraft would experience uncommanded lateral activity as a result of abrupt wing stall. However, no one specific figure of merit consistently flagged a warning of potential lateral activity when actual activity was seen to occur in the free-to-roll experiments. In fact, they yielded as many or more false indications of lateral activity than were seen in the free-to-roll response data. Excellent agreement between free-to-roll results and flight was obtained for those configurations where flight data were available.

If the experimental static figures of merit indicate a potential lateral activity, it is recommended to proceed to free-to-roll testing. It is essential that the free-to-roll test program include at least three test approaches: continuous sweep, pitch pause, and roll offsets. Some further refinement of free-to-roll test procedures are expected as further analysis of the results reaches completion. These studies pointed out the importance of measuring and recording the rms signals of the force balance. In addition, measurement of wing-bending moments is recommended because they can be directly compared to results obtained by computational methods.

References

¹Hall, R. M., and Woodson, S., "Introduction to the Abrupt Wing Stall (AWS) Program," AIAA Paper 2003-0589, Jan. 2003.

²Chambers, J. R., and Hall, R. M., "Historical Review of Uncommanded Lateral-Directional Motions at Transonic Speeds," AIAA Paper 2003-0590, Jan. 2003.

³Bore, C. L., "Post-Stall Aerodynamics of the Harrier," AGARD, CP-102, Nov. 1972.

⁴Capone, F. J., Owens, D. B., and Hall, R. M., "Development of a Free-to-Roll Transonic Test Capability," AIAA Paper 2003-0749, Jan. 2003.

⁵Ross, A. J., "Flying Aeroplanes in Buffet," *Aeronautical Journal*, Oct. 1977, pp. 427-436.

⁶Lamar, J. E., Capone, F. J., and Hall, R. M., "AWS Figures of Merit (FOM) Developed Parameters from Static, Transonic Model Tests," AIAA Paper 2003-0745, Jan. 2003.

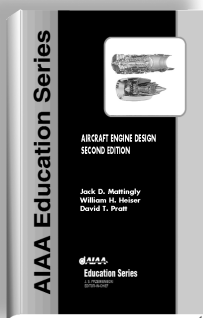
⁷Chung, J., and Parikh, P., "A Computational Study of the Abrupt Wing Stall (AWS) Characteristics for Various Fighter Jets, Part II, AV-8B and F/A-18C," AIAA Paper 2003-0747, Jan. 2003.

⁸Parikh, P., and Chung, J., "A Computational Study of the AWS Characteristics for Various Fighter Jets, Part I, F/A-18E & F-16C," AIAA Paper 2003-0746, Jan. 2003.

⁹Owens, D. B., Capone, F. J., Hall, R. M., Brandon, J., Cunningham, K., and Chambers, J. R., "Free-To-Roll Analysis of Abrupt Wing Stall on Military Aircraft at Transonic Speeds," AIAA Paper 2003-0750, Jan. 2003.

¹⁰Roesch, M., and Randall, B., "Flight Test Assessment of Lateral Activity," AIAA Paper 2003-0748, Jan. 2003.

¹¹Stevenson, S. W., Holl, D., and Roman, A., "Parameter Identification of AV-8B Wingborne Aerodynamics for Flight Simulator Model Updates," AIAA Paper 92-4506-CP, Aug. 1992.



AIRCRAFT ENGINE DESIGN, SECOND EDITION

Jack D. Mattingly—University of Washington • William H. Heiser—U.S. Air Force Academy • David T. Pratt—University of Washington

This text presents a complete and realistic aircraft engine design experience. From the request for proposal for a new aircraft to the final engine layout, the book provides the concepts and procedures required for the entire process. It is a significantly expanded and modernized version of the best selling first edition that emphasizes recent developments impacting engine design such as theta break/throttle ratio, life management, controls, and stealth. The key steps of the process are detailed in ten chapters that encompass aircraft constraint analysis, aircraft mission analysis, engine parametric (design point) analysis, engine performance (off-design) analysis, engine installation drag and sizing, and the design of inlets, fans, compressors, main combustors, turbines, afterburners, and exhaust nozzles.

The AEDsys software that accompanies the text provides comprehensive computational support for every design step. The software has been carefully integrated with the text to enhance both the learning process and productivity, and allows effortless transfer between British Engineering and SI units. The AEDsys software is furnished on CD and runs in the Windows operating system on PC-compatible systems. A user's manual is provided with the software, along with the complete data files used for the Air-to-Air Fighter and Global Range Airlifter design examples of the book.

2002, 692 pp, Hardback
ISBN: 1-56347-538-3
List Price: \$95.95
AIAA Member Price:
\$69.95

Contents:

- The Design Process
- Constraint Analysis
- Mission Analysis
- Engine Selection: Parametric Cycle Analysis
- Engine Selection: Performance Cycle Analysis
- Sizing the Engine: Installed Performance
- Engine Component Design: Global and Interface Quantities
- Engine Component Design: Rotating Turbomachinery
- Engine Component Design: Combustion Systems
- Engine Component Design: Inlets and Exhaust Nozzles
- Appendices

American Institute of Aeronautics and Astronautics
Publications Customer Service, P.O. Box 960, Herndon, VA 20172-0960
Fax: 703/661-1501 • Phone: 800/682-2422 • E-mail: warehouse@aiaa.org
Order 24 hours a day at www.aiaa.org



American Institute of Aeronautics and Astronautics

02-0545